PCCP

Accepted Manuscript

ROYAL SOCIETY OF CHEMISTRY

www.rsc.org/pccp

Journal Name

ARTICLE

Reactivity of Electrophilic Chlorine Atoms Due to σ-holes. A Mechanistic Assessment of the Chemical Reduction of the Trichloromethyl Group by Sulfur Nucleophiles

Received 00th January 20xx,
Accepted 00th January 20xx

DOI: 10.1039/x0xx00000x

www.rsc.org/

Guillermo Caballero-García,[a,b] Moisés Romero-Ortega[b] and Joaquín Barroso-Flores[a*]

σ-holes are shown to promote an electrophilic behavior on chlorine atoms in a trichloromethyl group when bound to an electron-withdrawing moiety. A halogen bond-type non-covalent interaction between a chlorine atom and a negatively charged sulfur atom takes place, causing the abstraction of such chlorine atom while leaving a carbanion, subsequently driving the chemical reduction of the trichloromethyl group to a sulfide in a stepwise process. The mechanism for the model reaction of trichloromethyl pyrimidine **1** with thiophenolate and thiophenol to yield phenylsulfide **4** was followed through ^{1}H-NMR and studied with DFT transition state calculations, the energy profile for this transformation is fully discussed. MP2 claculations of the electrostatic potential were performed for a series of trichloromethyl compounds in order to assess the presence of σ-holes and quantify them by means of the maximum surface electrostatic potential. Such calculations showed that the chlorine atoms behave as electrophilic leaving groups toward a nucleophilic attack, opening a new possibility in the synthetic chemistry of the trichloromethyl group.

Introduction

A σ-hole,[1–3] is conceived as a region of positive molecular electrostatic potential, which causes that seemingly negatively charged atoms interact with Lewis bases. In some cases, halogens -which are generally regarded to be negatively charged atoms, present an anisotropic electron density distribution- thus exhibiting a σ-hole, whose intensity depends on two main factors: the polarizability of the halogen atom (F<Cl<Br<I) and the electron-withdrawing power of the moiety to which the halogen is attached. An important consequence of this feature is the formation of halogen bonding,[4–11] which is generally regarded to be caused by the formation of a σ-hole.[12,13]

The σ-hole is located on the region of positive electrostatic potential opposite to the electron-withdrawing group (EWG) and along the EWG-X bond, *i.e.* over the halogen atom and opposite to the σ-bond. Not only halogens are capable of interacting with nucleophiles through σ-holes, but other atoms from groups III-VI as well.[14–19]

Among synthetic chemistry, the number of reactions, as well as theoretical studies, where halogen bonding is used as a driving force is increasing.[20–29] As an example, Huber *et al.* reported that a C-X (X=Br, Cl) cleavage was driven by a halogen bond formation using electron-deficient iodine atoms and a Lewis base.[30,31] These and other methodologies induce C-X bond cleavage where the halogen atom leaves as the corresponding halide.[32–37] To our knowledge, just few cases are reported,[38] albeit not fully discussed, where the halogen atom actually cleaves as a halonium-type leaving group yielding a carbanion, which is the case we herein discuss for a trichloromethyl group (Scheme 1). Moreover, chloronium-like abstraction is driven by the attack of a negatively charged sulfur atom rather than being promoted by a halogen-Lewis base complex.

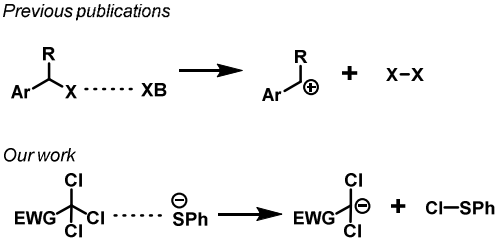

Scheme 1. Chloronium abstraction induced by the negatively charged sulfur atom in thiophenolate.

[a] Centro Conjunto de Investigación en Química Sustentable UAEM – UNAM. Carretera Toluca–Atlacomulco km 14.5, Unidad San Cayetano, personal de la UNAM, Toluca 50200, Estado de México, México. Email: jbarroso@unam.mx
[b] Facultad de Química, Universidad Autónoma del Estado de México, Paseo Colón/Paseo Tollocan, s/n Toluca 50000, Estado de México, México.

Electronic Supplementary Information (ESI) available: S1. Experimental Procedures and NMR data. S2. Full Gaussian and Image Processing software References. S3. Cartesian coordinates of optimized structures. S4. Calculated IRC paths for all transition states. S5. List of maximum surface electrostatic potentials. S6. References. See DOI: 10.1039/x0xx00000x

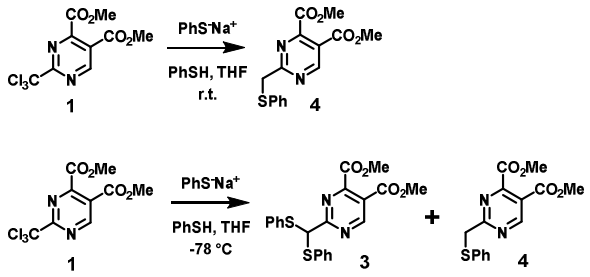

Scheme 2. Reactivity of trichloromethyl group with sulfur nucleophiles *i.e.* thiophenol and sodium thiophenolate.

Trichloromethyl group has been employed as a versatile synthetic tool, whether as a leaving group or as a chemical precursor for a variety of functional groups,[39–45] but when this group is bound to an electron-withdrawing system presents an unexpected behavior when reacts with sulfur nucleophiles. Previously, we reported that reaction of trichloromethylpyrimidine **1** (Scheme 2) with an excess of thiophenol and sodium thiophenolate yielded phenylsulfide **4** quantitatively under mild and straightforward conditions,[46,47] obtaining diphenyldisulfide as the only reaction by-product. When this reaction is carried out at -78 °C yields a mixture of the thioacetal **3** and the sulfide **4** (Scheme 2),[48] presumably passing through intermediate **2** (*vide infra*). In order to obtain **4**, protic media is required, coming from thiophenol. If only thiophenolate is present, compound **3** becomes the major product. Despite the fact that **3** is an intermediate compound *en route* to sulfide **4**, no explanation about the reaction mechanism has been reported. The versatility of the trichloromethyl group is, that not only sulfides are obtained from this reaction, but other compounds such as thioloesters, thioacetals or the dichloro compounds as well.[49–53]

Modern chemistry requires a synergic contribution form experiment and theory, thus the broad application of computational chemistry plays an important role in the investigation of reaction mechanisms.[54–60] Herein we prove that σ-holes located over the electronic isodensity surface of chlorine atoms in trichloromethyl compounds are a driving force to obtain sulfide **4** from trichloromethylpyrimidine **1**. The intensities of σ-holes are quantified through the maximum surface electrostatic potential values, which are easily calculated, to get insights for the reactivity of trichloromethyl group when attached to electron-withdrawing groups. Moreover, a reaction mechanism supported by DFT transition state (TS) calculations is presented for compound **1** in order to show how σ-hole interactions trigger the entire reaction to yield sulfide **4**.

Computational details

DFT calculations were performed with the Gaussian 09 Rev. D01 suite of programs.[61] Gas phase geometry optimizations were done with the Boese-Martin for kinetics BMK functional[62] and the split valence 6-31G(*d*,*p*) basis set.[63,64] This functional has been used for kinetic calculations, yielding good to excellent results for the study of organic reactions.[65–69] Frequencies at the aforementioned level of theory were calculated to verify that the optimized structures were energy minima or TSs. Only one imaginary frequency was found for the latter and none for the former. Temperature correction at -78 °C (195.15 K) is included in the thermochemical analysis, this is the temperature at which the experiments were performed.

Cartesian coordinates for all calculated structures are presented in the Electronic Supplementary Information (ESI).

The electrostatic potential was calculated at the MP2/cc-pVQZ level of theory[70,71] taking the previously optimized geometries in order to map it onto the isodensity surface. Dunning quadruple-ζ basis set[72–74] has proved to give the best results when used with MP2 calculations.[75] The values of maximum electrostatic potential over the isodensity surface were calculated with MultiWFN,[76,77] as an approach to quantifying the σ-holes.

Experimental

Reaction of **1** with thiophenol (5 equiv.) and sodium thiophenolate (5 equiv.) was performed at -78 °C and quenched at different reaction times (1, 5, 10, 30 and 90 minutes) in order to isolate any possible intermediate in the course of the reaction, after quenching, the products were jointly purified but isolated from thiophenol and diphenyldisulfide. Pyrimidine **1** was chosen as a model compound for this study because of the few NMR signals present, thus minimizing background noise or too much signal overlapping allowing us to use this tool for following the course of the reaction. Further details for the experimental procedures as well as NMR spectra are fully provided in the ESI (section S1).

Results and discussion

Before starting the reaction, spectrum of trichloromethylpyrimidine **1** was recorded as the reference for t = 0 (figure 1, black arrow at δ = 9.40 ppm). After one minute, it is observed that the aforementioned signal is gone, but two new peaks at 9.37 and 6.83 ppm are now present (figure 1, red arrows), indicating the formation of only one product. Such spectrum corresponds to the dichloromethylpyrimidine **2**, whose full NMR characterization is given in the ESI. A plausible manner to explain the formation of **2** is through the immediate protonation of the corresponding carbanion, which may be formed by a direct attack of the sulfur atom in thiophenolate to an electrophilic chlorine atom.

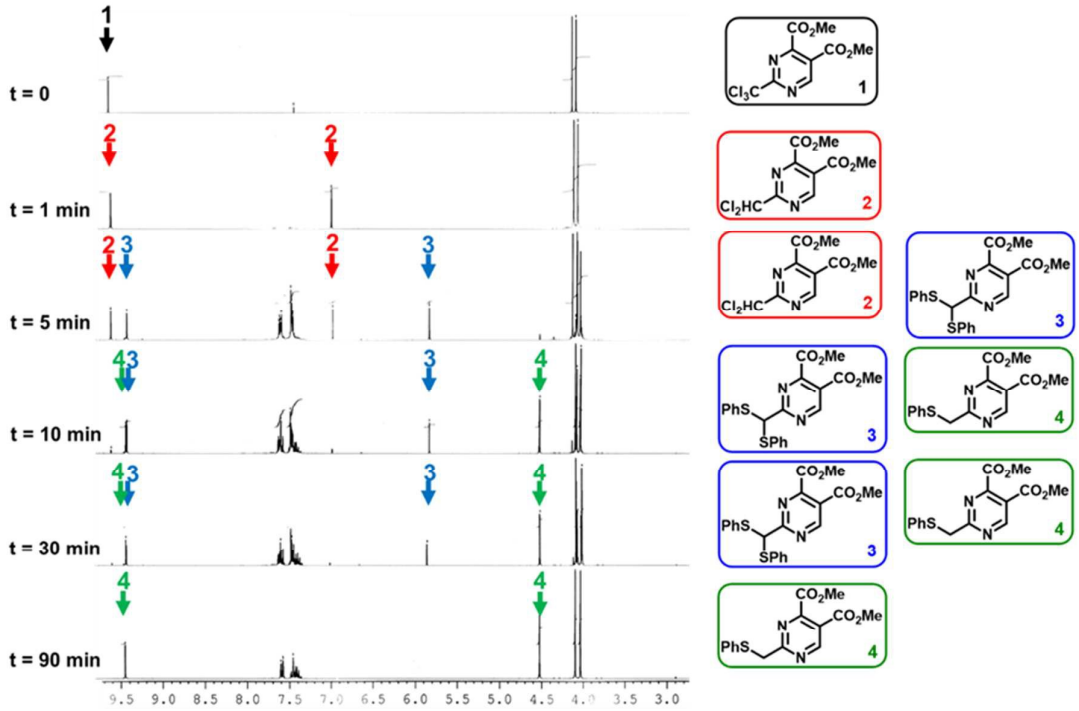

Figure 1. NMR reaction following at -78 °C. Colored arrows indicate the peaks that were followed for each compound: Black for trichloromethylpyrimidine **1**, red for dichloromethylpyrimidine **2**, blue for thioacetal **3** and green for sulfide **4**. Chemical shift is given in ppm. Times correspond to reaction time until quenching, not to real-time NMR following.

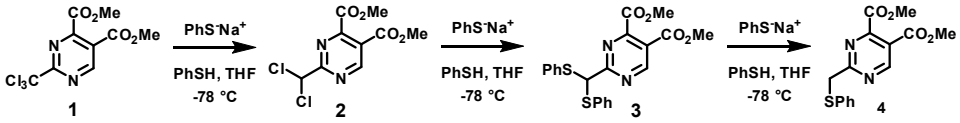

t /min	% **2**	% **3**	% **4**
1	100	0	0
5	43	57	0
10	0	45	55
30	0	33	67
90	0	0	100

Table 1. Percentage of compounds formed at 1, 5, 10, 30 and 90 minutes of reaction. Percentages were estimated from the NMR integrals. Times correspond to reaction time until quenching.

Subsequently, at t = 5 min, peaks in the aromatic region appear indicating that thiophenolate has incorporated to the compound. Two more signals appear at 9.18 ppm and 5.69 ppm corresponding to the formation of thioacetal **3** (figure 1, blue arrows). An approximately 1:1 ratio of **2** and **3** is observed at this time, suggesting that dichloro compound **2** reacts with the excess of sodium thiophenolate to yield thioacetal **3**. This suggests that **2** is the direct precursor of **3**.

After ten minutes, the peaks for **2** are no longer observed and one singlet integrating for two protons at 4.41 ppm, stating for a methylene moiety, indicates that sulfide **4** has appeared in the reaction media (figure 1, green arrows). A 1:1 mixture of thioacetal **3** and sulfide **4** is isolated. At 30 minutes, this ratio changes in favor of **4** (2:1). The percentage of each product in function of reaction time was estimated from the NMR integrals and are presented in table 1 with the suggested

sequence of intermediates. If the reaction is left at -78 °C for a longer reaction time (90 minutes), only sulfide **4** is isolated.

For compound **2** to be formed, a direct attack on a chlorine atom should be the first step of the reaction mechanism so the chlorine atoms behave as electrophiles when the trichloromethyl group is attached to an electron-withdrawing system. In order to test this hypothesis and assess if this mechanism can be extended to other trichloromethyl compounds, *ab initio* electrostatic potential calculations were performed at the MP2/cc-pVQZ level of theory for the analogous compounds shown in chart 1 (taken from the literature[47]) in order to assess the electrophilic character of chlorine atoms. The surface potential $V_S(\mathbf{r})$ was calculated at 0.001 au (e Bohr^{-3}) contour value as suggested by Bader *et al.*[78] since that one encompasses most of the molecule's van der Waals radii. We will focus in the most positive values of $V_S(\mathbf{r})$ located over the chlorine atoms, labeled $V_{S,max}$, to quantify the region of positive potential.

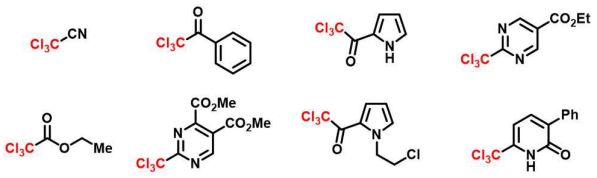

Chart 1. Trichloromethyl group bound to electron-withdrawing systems for which the $V_{S,max}$ was calculated.

In figure 2, the electrostatic potential mapped onto the isodensity surface (0.001 au) shows the presence of a σ-hole for each of the three chlorine atoms, including the calculated values for $V_{S,max}$ over each σ-hole. For these compounds, the $V_{S,max}$ values are positive, indicating the possibility to form halogen bonds with Lewis bases. Such interaction with negatively charged sulfur nucleophiles promotes an attack on the chlorine atom. This reaction only proceeds when the trichloromethyl group is bound to an electron-withdrawing moiety, otherwise, the starting materials are recovered unreacted; compounds in figure 2 are known to yield the corresponding sulfides when treated under the same reaction conditions as presented in scheme 2.[47]

In order to assess if other factors aside from σ-holes promote this reaction, we conducted a transition state-based mechanistic investigation on the transformation of compound **1** into **4** (Scheme 3).

In the first stage of the mechanism, a chlorine atom in **1** is nucleophilically attacked by a thiophenolate anion due to the presence of a σ-hole, yielding phenylsulfenylchloride and carbanion **6**. Due to the excess of sodium thiophenolate, phenylsulfenylchloride is attacked to form diphenyldisulfide. Intermediate carbanion **6** is immediately protonated by thiophenol yielding dichloromethylpyrimidine **2**. For this stage, **TS 1-6** (figure 3) the activation free energy was calculated to be 3.51 kcal mol^{-1} for the nucleophilc attack on the chlorine atom in order to form carbanion **6**.

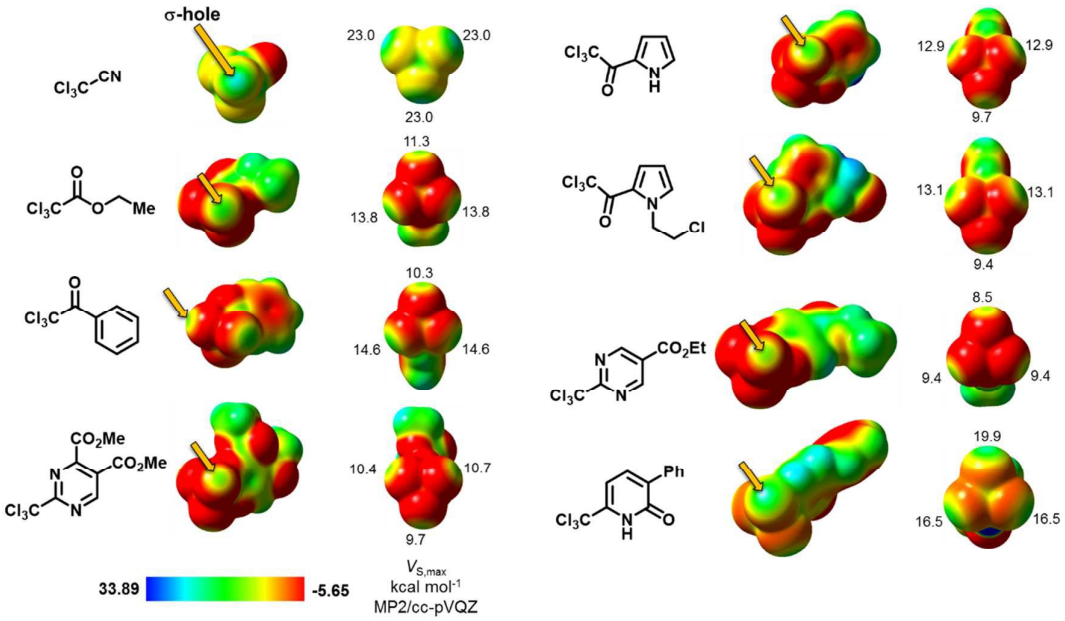

Figure 2. Electrostatic potential mapped onto the isodensity surface (0.001 au) for compounds in chart 1. Numbers are the $V_{S,max}$ values and are given in kcal mol^{-1}. Electrostatic potential was calculated at the MP2/cc-pVQZ level of theory taking the BMK/6-31G(*d*,*p*) optimized geometries.

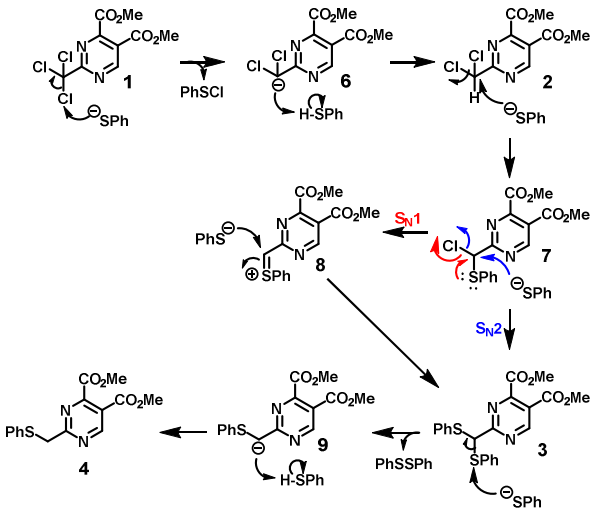

Scheme 3. Proposed reaction mechanisms to explain the formation of **4** from **1**.

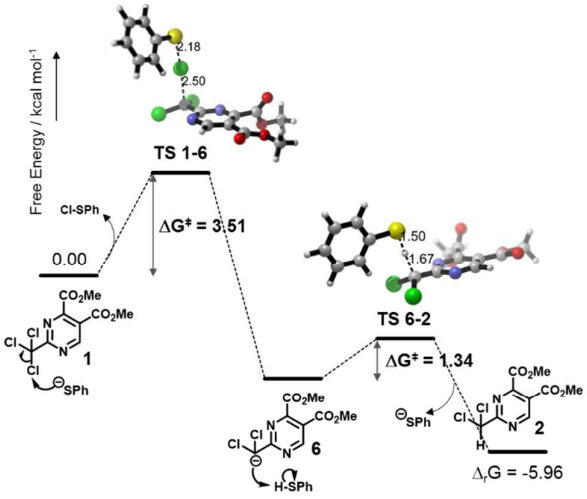

Figure 3. Energy profile for the transformation of **1** to **2**. Numbers are free energy values and are given in kcal mol^{-1}. Energies are relative to infinitely separated reagents for consistency on the total number of particles.

The energy profile, presented in figure 3, indicates that the first step corresponds to the rate-determining elementary step for this same stage, whereas the protonation proceeds with a significantly lower activation free energy (1.34 kcal mol^{-1} respect to **6**). The free reaction energy was calculated to be -5.96 kcal mol^{-1}. Reversibility does not occur because of the acidity of the proton in the dichloromethyl group which cannot be removed by thiophenolate (pK_a = 6).

This stage from **1** to **2** passing through **6** resembles an electrophilic aliphatic substitution (S_E1) promoted by the initial interaction of thiophenolate with the chlorine atom through a σ-hole present in **1**. This interaction triggers the attack on the chlorine atom in order to form carbanion **6**, which is highly stabilized by the electron-withdrawing heterocycle. Although the reaction is promoted by the σ-hole, the stability of the carbanion plays a crucial role, explaining why this reaction does not proceed if the trichloromethyl group is not bound to an electron-withdrawing moiety.

The energy profile for the second stage of the mechanism is depicted in figure 4. Once **2** is formed it undergoes an S_N2 attack by a thiophenolate molecule to yield **7**, this step requires an activation free energy of 8.56 kcal mol^{-1} (**TS 2-7**). At this point, the mechanism can follow two possible pathways: the first of which is simply another S_N2 reaction to yield thioacetal **3** in another elementary step *via* **TS 7-3** (6.57 kcal mol^{-1} relative to **7**). We suggest the second pathway might be an S_N1 reaction driven by chloride elimination assisted by a lone pair on the sulfur atom. The positively charged sulfur atom interacts with chloride forming an ionic pair as observed with the dotted line in **TS 7-8** (44.18 kcal mol^{-1} relative to **7**), followed by thiophenolate addition to **8** to yield **3** *via* **TS 8-3**).

The former pathway, through **TS 7-3**, has a lower free activation energy, suggesting that this is the most favorable pathway. In this stage, the formation of **3** is exergonic (Δ_rG = -17.70 kcal mol^{-1}).

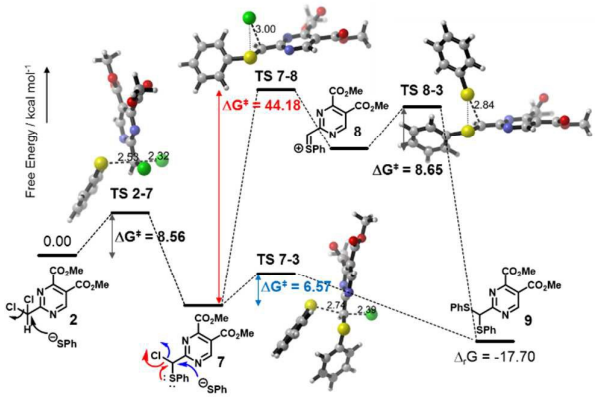

Figure 4. Energy profile for the transformation of **2** into **3**. Free energy values are given in kcal mol^{-1}. Energies are relative to infinitely separated reagents for consistency on the total number of particles.

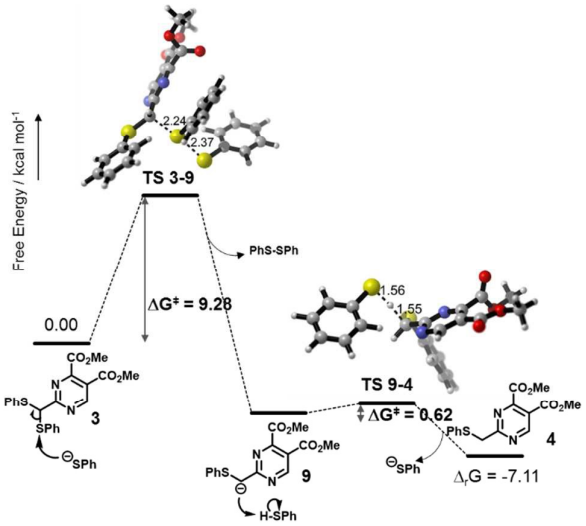

Figure 5. Energy profile for the transformation of **3** into **4**. Free energy values are given in kcal mol^{-1}. Energies are relative to infinitely separated reagents for consistency on the total number of particles.

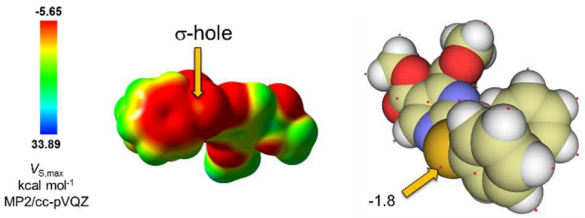

Figure 6. Electrostatic potential mapped onto the isodensity surface (0.001 au) for compound **3**. Numbers are the $V_{S,max}$ values and are given in kcal mol^{-1}.Electrostatic potential was calculated at the MP2/cc-pVQZ level of theory taking the BMK/6-31G(*d*,*p*) optimized geometry. Red dots indicate the position of $V_{S,max}$.

The last stage of the mechanism *en route* to **4** is similar to the first one (figure 5). In order to reach **TS 3-9** (9.28 kcal mol^{-1}) a thiophenolate molecule attacks a sulfur atom within the thioacetal moiety to yield carbanion **9** and another equivalent of diphenyldisulfide. Once the carbanion **9** is formed it is readily protonated by thiophenol (**TS 9-4**, 0.62 kcal mol^{-1}) to finally yield sulfide **4**.

From the electrostatic potential mapped onto the isodensity surface for thioacetal **3** (Figure 6) it is suggested that the attack over a sulfur atom in thioacetal **3** may also promoted both by a σ-hole interaction with the sulfur atom in thiophenolate and the high stability of the forming carbanion. The weaker intensity of the σ-hole correlates well with the quite longer reaction time to finally yield **4**.

We also analyzed the possibility to obtain the fully reduced product from **1**, reducing the trichoromethyl group to a methyl group using thiophenol and sodium thiophenolate, albeit this total reduction is reported to be carried out by means of catalytic hydrogenation. When the reaction was done at THF reflux temperature (*ca*. 50-65 °C) for 24 hours, sulfide **4** is isolated. Longer reaction time (7 days) at reflux yields about 5% of methylpyrimidine **5** (Figure 7). This is inferred by observing a peak at 2.84 ppm in the ^{1}H NMR spectrum (ESI, section S1). Despite the fact that the yield of this very last stage is low, the total reduction of a trichloromethyl to a methyl group is possible, although difficult under these reaction conditions.

A mechanism with its corresponding energy profile, presented in figure 7, is also proposed from compound **4** to yield **5**. The sulfur atom in **4** is attacked by a thiophenolate molecule to form carbanion **10**, which protonates to afford methylpyrimidine **5**. TSs for this mechanism were calculated to evaluate its feasibility. To reach **TS 4-10** from **4**, 19.03 kcal mol^{-1} are needed, explaining the low yield for this transformation to occur, even when the protonation step is less energetic (0.40 kcal mol^{-1}).

To gain insight about the high barrier for **TS 4-10**, the electrostatic potential for **4** was calculated to see the presence or absence of a σ-hole that could trigger this attack (figure 8). No σ-hole is observed on the sulfur atom and the negative value of $V_{S,max}$ (-3.37 kcal mol^{-1}) indicates that this sulfur atom behaves merely as a nucleophile, with no possibility of interaction with the negatively charged sulfur atom in a thiophenolate molecule.

Taking everything into account, the full energy profile for the chemical reduction of **1** using thiophenol and thiophenolate is presented in figure 9. From the activation free energies, it is shown that the whole reaction from **1** to **4** is both thermodynamically favored and kinetically accessible.

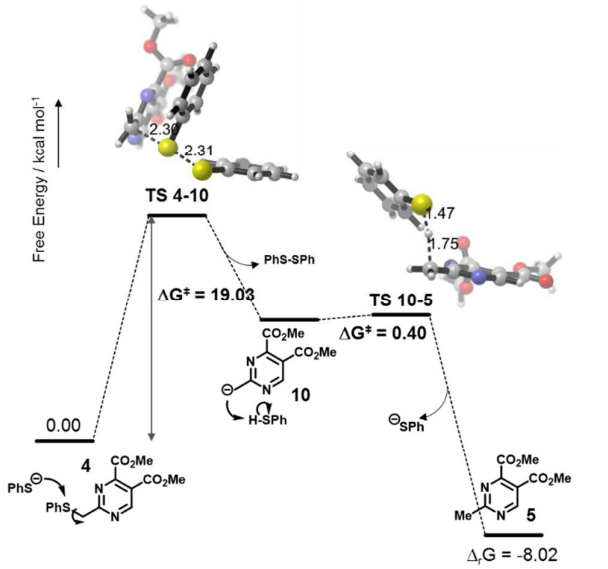

Figure 7. Energy profile for the transformation of **4** into **5**. Numbers are free energy values and are given in kcal mol^{-1}. Energies are relative to infinitely separated reagents for consistency on the total number of particles.

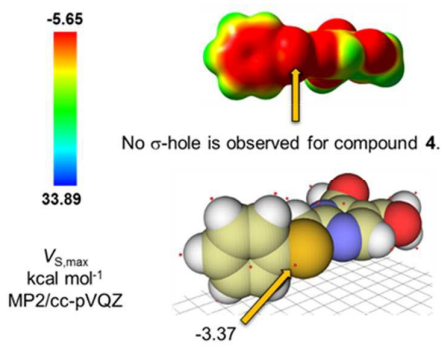

Figure 8. Electrostatic potential mapped onto the isodensity surface (0.001 au) for compound **4**. Electrostatic potential was calculated at the MP2/cc-pVQZ level of theory taking the BMK/6-31G(*d*,*p*) optimized geometry. No σ-holes are observed.

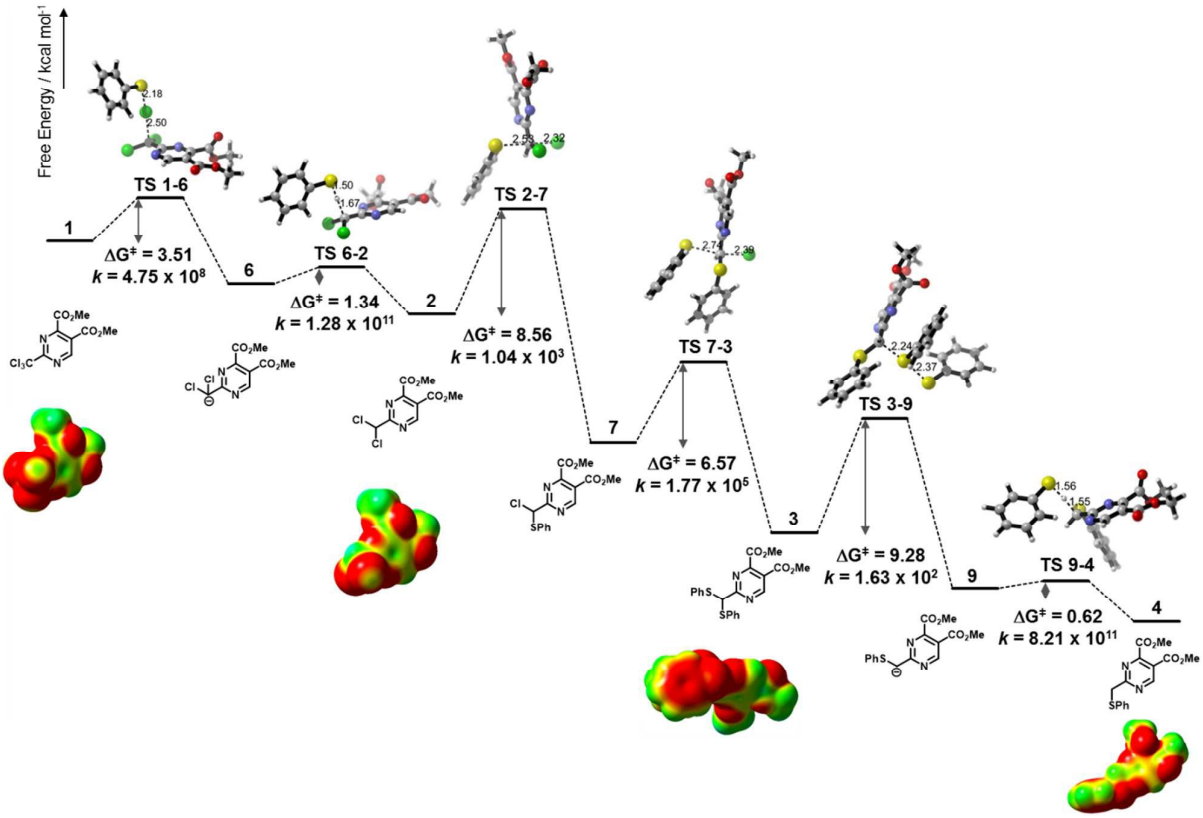

Figure 9. Full energy profile for the chemical reduction of trichloromethyl pyrimidine **1** to phenylsulfide **4**. Numbers are free energy values relative to the starting materials and are given in kcal mol^{-1}. Energies are relative to infinitely separated reagents for consistency on the total number of particles. Rate constants are given in s^{-1}. Only key structures are presented for simplicity. Mapped electrostatic potentials for compounds **1**, **2**, **3** and **4** are also shown.

Conclusions

DFT calculations indicate that the chemical reduction of trichloromethyl compounds with thiophenol and sodium thiophenolate proceeds via the mechanism suggested herein (scheme 3 and figure 9). The first nucleophilic attack proceeds over a chlorine atom in the trichloromethyl group further leading to the corresponding dichloromethyl compound, which undergoes two consecutive S_N2 reactions to yield a thioacetal which continues reacting yielding a phenylsulfide. This reaction

proved to be both thermodynamically favored as well as kinetically accessible (highest $\Delta G^{\ddagger}$ = 9.28 kcal mol^{-1}).

MP2 calculations suggest that the first step in the mechanism is promoted by a σ-hole over the chlorine atoms of the trichloromethyl group. The positive values of the calculated $V_{S,max}$ indicate that such chlorine atoms behave as electrophiles toward the nucleophilic sulfur atom in thiophenolate (figure 2).

σ-holes can be used as an advantageous synthetic tool, for example, compound **2** is a possible target for developing a methodology to obtain it from a trichloromethyl group and use it as a carbene precursor.

Acknowledgements

We thank DGTIC-UNAM for the access provided to Miztli supercomputer and María de las Nieves Zavala-Segovia for recording all NMR spectra, to Citlalit Martínez for keeping our computing services running and to Dr. Nelly González-Rivas for her assistance.

Notes and references

1 P. Politzer, J. S. Murray and M. C. Concha, *J. Mol. Model.*, 2008, **14**, 659–665.

2 J. S. Murray, P. Lane and P. Politzer, *J. Mol. Model.*, 2009, **15**, 723–9.

3 J. S. Murray, P. Lane, T. Clark, K. E. Riley and P. Politzer, *J. Mol. Model.*, 2012, **18**, 541–548.

4 G. Cavallo, P. Metrangolo, R. Milani, T. Pilati, A. Priimagi, G. Resnati and G. Terraneo, *Chem. Rev.*, 2016, **116**, 2478–2601.

5 M. H. Kolář and P. Hobza, *Chem. Rev.*, 2016, **116**, 5155–5187.

6 J. S. Murray, P. Lane and P. Politzer, *Int. J. Quantum Chem.*, 2007, **107**, 2286–2292.

7 P. Politzer, J. S. Murray and T. Clark, *Phys. Chem. Chem. Phys.*, 2013, **15**, 11178–11189.

8 P. Politzer, J. S. Murray and T. Clark, *Phys. Chem. Chem. Phys.*, 2010, **12**, 7748.

9 T. Clark, M. Hennemann, J. S. Murray and P. Politzer, *J. Mol. Model.*, 2007, **13**, 291–296.

10 K. Eskandari and M. Lesani, *Chem. - A Eur. J.*, 2015, **21**, 4739–4746.

11 M. R. Scholfield, C. M. Vander Zanden, M. Carter and P. S. Ho, *Protein Sci.*, 2013, **22**, 139–152.

12 P. Politzer, J. S. Murray and T. Clark, *Top. Curr. Chem.*, 2015, **358**, 19–42.

13 A. Bauza, T. J. Mooibroek and A. Frontera, *ChemPhysChem*, 2015, **16**, 2496–2517.

14 J. S. Murray, P. Lane, T. Clark and P. Politzer, *J. Mol. Model.*, 2007, **13**, 1033–8.

15 J. Ji, Y. Zeng, X. Zhang, S. Zheng and L. Meng, *J. Mol. Model.*, 2013, **19**, 4887–4895.

16 A. Bauza, T. J. Mooibroek and A. Frontera, *ChemPhysChem*, 2016, Ahead of Print.

17 L. Gao, Y. Zeng, X. Zhang and L. Meng, *J. Comput. Chem.*, 2016, **37**, 1321–1327.

18 M. D. Esrafili and F. Mohammadian-Sabet, *Struct. Chem.*, 2016, **27**, 617–625.

19 W. Li, Y. Zeng, X. Li, Z. Sun and L. Meng, *J. Comput. Chem.*, 2015, **36**, 1349–1358.

20 M. Breugst, E. Detmar and D. von der Heiden, *ACS Catal.*, 2016, **6**, 3203–3212.

21 A. Bruckmann, M. A. Pena and C. Bolm, *Synlett*, 2008, 900–902.

22 O. Coulembier, F. Meyer and P. Dubois, *Polym. Chem.*, 2010, **1**, 434.

23 V. de P. N. Nziko and S. Scheiner, *J. Org. Chem.*, 2016, **81**, 2589–2597.

24 Y. Takeda, D. Hisakuni, C.-H. Lin and S. Minakata, *Org. Lett.*, 2015, **17**, 318–321.

25 M. Saito, N. Tsuji, Y. Kobayashi and Y. Takemoto, *Org. Lett.*, 2015, **17**, 3000–3003.

26 S. H. Jungbauer, S. M. Walter, S. Schindler, L. Rout, F. Kniep and S. M. Huber, *Chem. Commun.*, 2014, **50**, 6281.

27 W. He, Y. C. Ge and C. H. Tan, *Org. Lett.*, 2014, **16**, 3244–3247.

28 S. J. Grabowski, *Phys. Chem. Chem. Phys.*, 2015, **17**, 13539–13546.

29 S. J. Grabowski, *Phys. Chem. Chem. Phys.*, 2014, **16**, 1824–1834.

30 S. M. Walter, F. Kniep, E. Herdtweck and S. M. Huber, *Angew. Chemie - Int. Ed.*, 2011, **50**, 7187–7191.

31 F. Kniep, S. H. Jungbauer, Q. Zhang, S. M. Walter, S. Schindler, I. Schnapperelle, E. Herdtweck and S. M. Huber, *Angew. Chemie Int. Ed.*, 2013, **52**, 7028–7032.

32 S. H. Jungbauer and S. M. Huber, *J. Am. Chem. Soc.*, 2015, **137**, 12110–12120.

33 N. Tsuji, Y. Kobayashi and Y. Takemoto, *Chem. Commun. (Camb).*, 2014, **50**, 13691–4.

34 F. Kniep, S. M. Walter, E. Herdtweck and S. M. Huber, *Chem. - A Eur. J.*, 2012, **18**, 1306–1310.

35 F. Kniep, L. Rout, S. M. Walter, H. K. V. Bensch, S. H. Jungbauer, E. Herdtweck and S. M. Huber, *Chem. Commun.*, 2012, **48**, 9299–9301.

36 J. Xie, M. McClellan, R. Sun, S. C. Kohale, N. Govind and W. L. Hase, *J. Phys. Chem. A*, 2015, **119**, 817–825.

37 J. Xie, R. Sun, M. R. Siebert, R. Otto, R. Wester and W. L. Hase, *J. Phys. Chem. A*, 2013, **117**, 7162–7178.

38 M. Ballester, C. Molinet and J. Rosa, *Tetrahedron*, 1959, **6**, 109–122.

39 H. G. Bonacorso, R. V Lourega, A. D. Wastowski, A. F. C. Flores, N. Zanatta and M. A. P. Martins, *Tetrahedron Lett.*, 2002, **43**, 9315–9318.

40 M. Romero-Ortega, A. Aviles, R. Cruz, A. Fuentes, R. M. Gómez and A. Plata, *J. Org. Chem.*, 2000, **65**, 7244–7247.

41 M. A. P. Martins, A. F. C. Flores, G. P. Bastos, A. Sinhorin, H. G. Bonacorso and N. Zanatta, *Tetrahedron Lett.*, 2000, **41**, 293–297.

42 E. Anders, A. Opitz, K. Wermann, B. Wiedel, M. Walther, W. Imhof and H. Goerls, *J. Org. Chem.*, 1999, **64**, 3113–3121.

43 M. Mattioli, P. Mencarelli and F. Stegel, *J. Org. Chem.*,

1988, **53**, 1087–1088.
44 R. S. Dainter, H. Suschitzky and B. J. Wakefield, *Tetrahedron Lett.*, 1984, **25**, 5693–5696.
45 E. C. Chukovskaya, R. K. Freidlina and N. A. Kuz'mina, *Synthesis (Stuttg).*, 1983, 773–784.
46 A. Guzmán, M. Romero, F. X. Talamás and J. M. Muchowski, *Tetrahedron Lett.*, 1992, **33**, 3449–3452.
47 M. Romero-Ortega, A. Fuentes, C. González, D. Morales and R. Cruz, *Synthesis (Stuttg).*, 1999, **1999**, 225–227.
48 A. Guzmán, M. Romero, F. X. Talamás, R. Villena, R. Greenhouse and J. M. Muchowski, *J. Org. Chem.*, 1996, **61**, 2470–2483.
49 E. Kober, *J. Org. Chem.*, 1961, **26**, 2270–2273.
50 Y. Sawama, T. Imanishi, R. Nakatani, Y. Fujiwara, Y. Monguchi and H. Sajiki, *Tetrahedron*, 2014, **70**, 4540–4546.
51 M. Nagao, N. Sato, T. Akashi and T. Yoshida, *J. Am. Chem. Soc.*, 1966, **88**, 3447–3449.
52 M. Romero-Ortega, H. Reyes, A. Covarruvias-Zuñiga, R. Cruz and J. G. Avila-Zarraga, *Synthesis (Stuttg).*, 2003, **2003**, 2765–2767.
53 N. G. Rivera, D. C. Becerril, C. Guadarrama-Pérez, A. Covarrubias-Zuñiga, J. G. Avila-Zárraga and M. Romero-Ortega, *Tetrahedron Lett.*, 2007, **48**, 1201–1204.
54 J. Mikosch, S. Trippel, C. Eichhorn, R. Otto, U. Lourderaj, J. X. Zhang, W. L. Hase, M. Weidemüller and R. Wester, *Science*, 2008, **319**, 183–6.
55 T. Sperger, I. A. Sanhueza, I. Kalvet and F. Schoenebeck, *Chem. Rev. (Washington, DC, United States)*, 2015, **115**, 9532–9586.
56 E. Soriano and I. Fernandez, *Chem. Soc. Rev.*, 2014, **43**, 3041–3105.
57 M. W. Lodewyk, M. R. Siebert and D. J. Tantillo, *Chem. Rev. (Washington, DC, United States)*, 2012, **112**, 1839–1862.
58 J. Gao, S. Ma, D. T. Major, K. Nam, J. Pu and D. G. Truhlar, *Chem. Rev. (Washington, DC, United States)*, 2006, **106**, 3188–3209.
59 P. Geerlings, F. De Proft and W. Langenaeker, *Chem. Rev. (Washington, DC, United States)*, 2003, **103**, 1793–1873.
60 A. Hameed, S. T. Zehra, S. Abbas, R. U. Nisa, T. Mahmood, K. Ayub, M. Al-Rashida, J. Bajorath, K. M. Khan and J. Iqbal, *Bioorg. Chem.*, 2016, **65**, 38–47.
61 D. J. Frisch, M. J.; Trucks, G. W.; Schlegel, H. B.; Scuseria, G. E.; Robb, M. A.; Cheeseman, J. R.; Scalmani, G.; Barone, V.; Mennucci, B.; Petersson, G. A.; Nakatsuji, H.; Caricato, M.; Li, X.; Hratchian, H. P.; Izmaylov, A. F.; Bloino, J.; Zheng, G.; Sonnenb, 2009.
62 A. D. Boese and J. M. L. Martin, *J. Chem. Phys.*, 2004, **121**, 3405–16.
63 R. Ditchfield, *J. Chem. Phys.*, 1971, **54**, 724.
64 V. A. Rassolov, M. A. Ratner, J. A. Pople, P. C. Redfern and L. A. Curtiss, *J. Comput. Chem.*, 2001, **22**, 976–984.
65 A. G. Vandeputte, M.-F. Reyniers and G. B. Marin, *Theor. Chem. Acc.*, 2009, **123**, 391–412.
66 M. E. Segovia, K. Irving and O. N. Ventura, *Theor. Chem. Acc.*, 2013, **132**, 1301.
67 T. M. El-Gogary and A. M. El-Nahas, *J. Mol. Struct. THEOCHEM*, 2008, **851**, 54–62.
68 Q. Zhang, K. Kawasumi, Y. Segawa, K. Itami and L. T. Scott, *J. Am. Chem. Soc.*, 2012, **134**, 15664–15667.
69 A. Galano and J. R. Alvarez-Idaboy, *J. Comput. Chem.*, 2014, **35**, 2019–26.
70 C. Møller and M. S. Plesset, *Phys. Rev.*, 1934, **46**, 618–622.
71 M. J. Frisch, M. Head-Gordon and J. A. Pople, *Chem. Phys. Lett.*, 1990, **166**, 275–280.
72 T. H. Dunning, *J. Chem. Phys.*, 1989, **90**, 1007.
73 D. E. Woon and T. H. Dunning, *J. Chem. Phys.*, 1993, **98**, 1358.
74 R. A. Kendall, T. H. Dunning and R. J. Harrison, *J. Chem. Phys.*, 1992, **96**, 6796.
75 E. Papajak and D. G. Truhlar, *J. Chem. Phys.*, 2012, **137**, 064110.
76 T. Lu and F. Chen, *J. Comput. Chem.*, 2012, **33**, 580–592.
77 T. Lu and F. Chen, *J. Mol. Graph. Model.*, 2012, **38**, 314–323.
78 R. F. W. Bader, M. T. Carroll, J. R. Cheeseman and C. Chang, *J. Am. Chem. Soc.*, 1987, **109**, 7968–7979.